Search for a bound state of $\Lambda_c\bar{\Sigma}_c$ near threshold

M. Ablikim *et al.*[*]
(BESIII Collaboration)

(Received 26 August 2025; accepted 29 October 2025; published 26 December 2025)

We search for a possible $\Lambda_c\bar{\Sigma}_c$ bound state, denoted as $H_c^{\pm}$, via the $e^+e^- \to \pi^+\pi^-\Lambda_c^+\bar{\Lambda}_c^-$ process for the first time. This analysis utilizes 207.8 and 159.3 pb^{-1} of e^+e^- annihilation data at the center-of-mass energies of 4918.02 and 4950.93 MeV, respectively, collected with the BESIII detector at the BEPCII collider. No statistically significant signal is observed. The upper limits of the product of Born cross section and branching fraction $\sigma(e^+e^- \to \pi^+H_c^- + \text{c.c.}) \times \mathcal{B}(H_c^- \to \pi^-\Lambda_c^+\bar{\Lambda}_c^-)$ at a 90% confidence level are reported at each energy point and for various H_c mass hypotheses (4715, 4720, 4725, 4730, and 4735 MeV/c^2) and widths (5, 10, or 20 MeV), with the upper limits ranging from 1.1 pb to 6.4 pb.

DOI: 10.1103/jv3m-h997

I. INTRODUCTION

Over the past decades, numerous hadron states and resonant structures have emerged in experimental data. Many of these discoveries deviate from the conventional quark-antiquark or three-quark hadron expectations from the quark model, and are likely evidence for exotic states such as multiquark states, hadronic molecules, hybrids, or glueballs [1]. Understanding their nature is crucial for advancing our knowledge of QCD. A notable feature of these states is their tendency to cluster near the thresholds of heavy-antiheavy hadron pairs. Prominent examples include the $X(3872)$ [also known as $\chi_{c1}(3872)$] [2] and the $Z_c(3900)^{\pm}$ [also known as $T_{c\bar{c}1}(3900)^{\pm}$] [3], which are situated near the $D\bar{D}^*$ threshold. These resonant structures have been extensively studied in various models, with many being interpreted as molecular states within their respective systems [4]. Among the related structures predicted to exist near the thresholds of heavy-antiheavy hadron pairs is the $\Lambda_c\bar{\Sigma}_c$ bound state a particularly intriguing candidate, consisting of a charmed baryon and an anticharmed baryon 5]]. It is predicted to exist with $(I, S) = (1, 0)$ and $J^{PC} = (0, 1)^{-\pm}$ [6]. However, no such bound state has been experimentally observed to date.

In this paper, the process $e^+e^- \to \pi^+\pi^-\Lambda_c^+\bar{\Lambda}_c^-$ has been used to search for a bound state of $\Lambda_c\bar{\Sigma}_c$, denoted $H_c^{\pm}$, decaying into $\pi^{\pm}\Lambda_c^+\bar{\Lambda}_c^-$. Charge-conjugated modes are implied throughout this paper. The analysis utilizes two data samples at the center-of-mass (c.m.) energies $\sqrt{s} =$ 4918.02 and 4950.93 MeV, corresponding to integrated luminosities of 207.8 ± 1.1 and 159.3 ± 0.9 pb^{-1} [7], respectively.

II. BESIII DETECTOR AND MONTE CARLO SIMULATION

The BESIII detector [8] records symmetric e^+e^- collisions provided by the BEPCII storage ring [9], which operates with a peak luminosity of 1.1×10^{33} cm^{-2} s^{-1} in the c.m. energy range from 1.84 to 4.95 GeV. The cylindrical core of the BESIII detector covers 93% of the full solid angle and consists of a helium-based multilayer drift chamber (MDC), a plastic scintillator time-of-flight system (TOF), and a CsI(Tl) electromagnetic calorimeter (EMC), which are all enclosed in a superconducting solenoidal magnet providing a 1.0 T magnetic field. The solenoid is supported by an octagonal flux-return yoke with resistive plate counter muon identification modules interleaved with steel. The charged-particle momentum resolution at 1 GeV/c is 0.5%, and the dE/dx resolution is 6% for electrons from Bhabha scattering. The EMC measures photon energies with a resolution of 2.5% (5%) at 1 GeV in the barrel (end cap) region. The time resolution in the TOF barrel region is 68 ps, while that in the end cap region is 110 ps. The end cap TOF system was upgraded in 2015 using multigap resistive plate chamber technology, providing a time resolution of 60 ps [10–12].

Simulated data samples are produced with a Geant4-based [13] Monte Carlo (MC) package, which includes the geometric description of the BESIII detector and the detector response [14]. They are used to optimize the event selection criteria and estimate the signal efficiency and the level of background. The simulation models the beam-energy spread and initial-state radiation (ISR) in the e^+e^-

[*]Full author list given at the end of the article.

Published by the American Physical Society under the terms of the Creative Commons Attribution 4.0 International license. Further distribution of this work must maintain attribution to the author(s) and the published article's title, journal citation, and DOI. Funded by SCOAP[3].

annihilation using the generator KKMC [15]. The inclusive MC sample, which consists of $\Lambda_c^+\bar{\Lambda}_c^-$ events, $D_{(s)}$ production, ψ states produced in initial state radiation processes, and continuum processes $e^+e^- \to q\bar{q}(q = u, d, s)$, are generated to estimate the potential background. Here, all the known decay modes of charmed hadrons and charmonia are modeled with EVTGEN [16,17] using branching fractions (BFs) taken from the Particle Data Group (PDG) [18], while the remaining unknown decays are modeled with LUNDCHARM [19,20]. Final state radiation from charged final state particles is incorporated using the PHOTOS package [21]. Given that the mass thresholds for the $\pi\Lambda_c\bar{\Lambda}_c$ and $\Lambda_c\bar{\Sigma}_c$ systems are 4710 MeV/c^2 and 4740 MeV/c^2, respectively, we set the H_c mass to the values 4715, 4720, 4725, 4730, and 4735 MeV/c^2, each with widths of 5, 10, or 20 MeV. For each of these 15 mass-width combinations, 60,000 MC events are simulated at each of the two energy points. The signal MC samples simulate the process $e^+e^- \to \pi^+H_c^-$, $H_c^- \to \pi^-\Lambda_c^+\bar{\Lambda}_c^-$, where the $\bar{\Lambda}_c^-$ decays generically while the Λ_c^+ decays into $pK^-\pi^+$. The decays of the signal process are modeled with a uniform phase space distribution, except for $\Lambda_c^+ \to pK^-\pi^+$, which uses the result from a partial wave analysis [22].

III. DATA ANALYSIS

A partial reconstruction method is applied for the signal process $e^+e^- \to \pi^+H_c^-$, $H_c^- \to \pi^-\Lambda_c^+\bar{\Lambda}_c^-$ to achieve a higher efficiency. The Λ_c^+ is reconstructed using the "Golden Mode" $\Lambda_c^+ \to pK^-\pi^+$ [23]. If an additional π is identified, the recoil mass of the π is calculated; otherwise the kinematic information of the reconstructed Λ_c^+ will be used to identify the signal.

Charged tracks detected in the MDC are required to be within a polar angle (θ) range of $|\cos\theta| < 0.93$, where θ is defined with respect to the z-axis (the symmetry axis of the MDC). The distance of the closest approach to the interaction point (IP) for charged tracks is required to be ± 10 cm along the z-axis and 1 cm in the plane perpendicular to the beam. Particle identification (PID) is implemented by combining measurements of the specific ionization energy loss in the MDC and the TOF between the IP and the dedicated TOF detector system. Each charged track is assigned to be a pion, kaon, or proton, according to which assignment has the highest probability.

The Λ_c^+ candidates are reconstructed by looping over all combinations of $pK^-\pi^+$ that satisfy a vertex fit, with a χ^2 value from the vertex fit less than 200. We require the $pK^-\pi^+$ invariant mass, denoted as $M(pK^-\pi^+)$, to be within the mass window $[2.270, 2.300]$ GeV/c^2 [24]. If multiple Λ_c^+ candidates are found within a single event, the one with the minimum χ^2 value is retained. For any

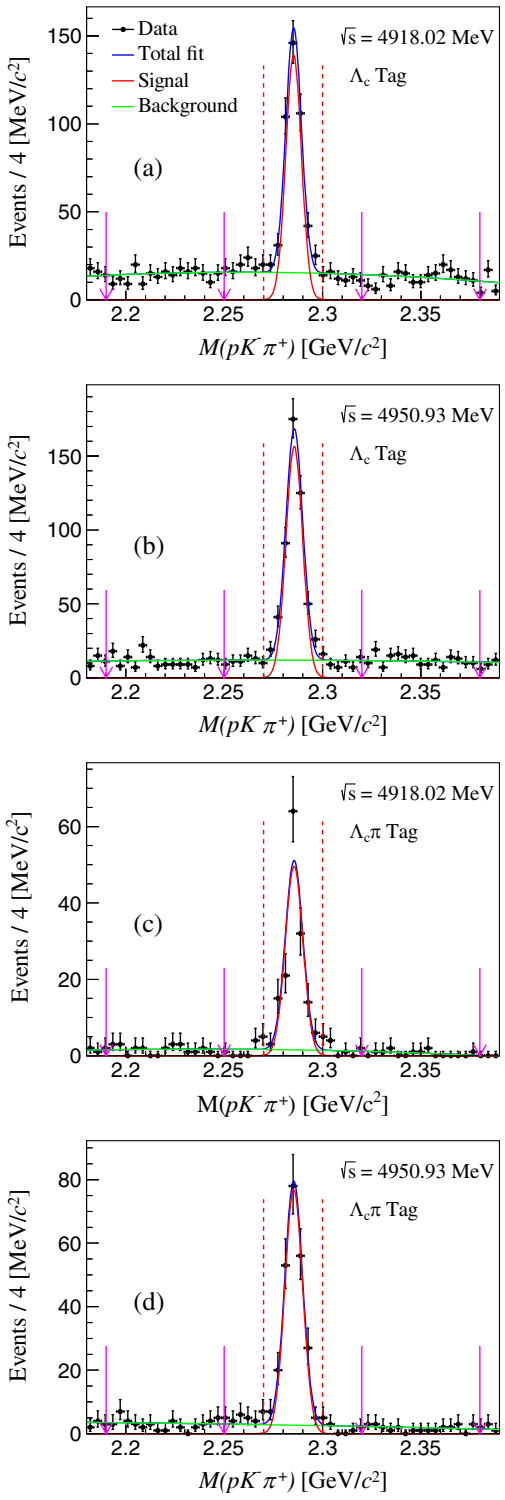


FIG. 1. The $M(pK^-\pi^+)$ distributions for "Λ_c Tag" events [(a), (b)] and "$\Lambda_c\pi$ Tag" events [(c), (d)] at $\sqrt{s} = 4918.02$ [(a), (c)] and 4950.93 MeV [(b), (d)]. The blue lines are the sum of the fit functions, the red lines indicate the signal, and the green lines are the background. The region between the red dashed lines is the Λ_c^+ signal region, and the regions between the two neighboring pink arrows are the Λ_c^+ sideband regions.

remaining π^+ or π^- particles, a vertex fit is performed to the $\Lambda_c^+\pi^+$ or $\Lambda_c^+\pi^-$ combinations, with a requirement that the χ^2 of the vertex fit is also less than 200. If multiple $\Lambda_c^+\pi^+$ or $\Lambda_c^+\pi^-$ combinations exist, we select the one with the minimum χ^2. If an event contains both $\Lambda_c^+\pi^+$ and $\Lambda_c^+\pi^-$ combinations, both are retained, as the signal process involves both $\pi^+H_c^-$ and $\pi^-H_c^+$ by charge conjugation. We select the combination with the best vertex fit to reduce the long-lived particles, Λ and K_S, in the Λ_c decay channels. Events that contain only Λ_c^+ and no other π are labeled as "Λ_c Tag," while those that include an extra π are designated as "$\Lambda_c\pi$ Tag." The distributions of $M(pK^-\pi^+)$ for the two tags are shown in Fig. 1, where evident Λ_c^+ signals are observed at both c.m. energies.

In addition, we have studied "$\Lambda_c\pi\pi$ Tag" events, which require at least one pair of $\pi^+\pi^-$ besides Λ_c^+ candidates. However, the reconstruction efficiency is very low due to the low momentum of the π. Therefore, the mode is not used afterward.

To determine the Born cross section (σ) of the signal process, an unbinned maximum likelihood fit is performed simultaneously on the two types of tagged events at each energy point. Explicitly, the fit comprises two categories:

(a) For the "Λ_c Tag" events, the single variable $RM(\Lambda_c^+) + M(\Lambda_c^+) - m(\Lambda_c^+)$ is used in the fit, where $RM(\Lambda_c^+)$ is the recoiling mass against the reconstructed Λ_c^+ in the c.m. system, $M(\Lambda_c^+)$ is the mass of the reconstructed Λ_c^+, and m(Λ_c^+) is the known Λ_c^+ mass from the PDG;

(b) For the "$\Lambda_c\pi$ Tag" events, the fit is two-dimensional, using the two variables $RM(\Lambda_c^+\pi^\pm) + M(\Lambda_c^+) - m(\Lambda_c^+)$ and $RM(\pi^\pm)$, where $RM(\Lambda_c^+\pi^\pm)$ and $RM(\pi^\pm)$ are the recoiling mass against the selected $\Lambda_c^+\pi^\pm$ system and the $\pi^\pm$, respectively.

The background components are categorized into two classes:

(a) Contributions from $e^+e^- \to q\bar{q}$ processes. These are described using the sideband regions of the $M(pK^-\pi^+)$ distribution in the data, as shown in Fig. 1. The signal region is the same as the Λ_c^+ mass window, and the sideband regions are [2.190, 2.250] and [2.320, 2.380] GeV/c^2. To determine the number of background events, we fit this distribution. A Gaussian function, along with a second-order Chebyshev polynomial, is used to fit the $M(pK^-\pi^+)$ distribution in data, representing the signal and background contributions, respectively.

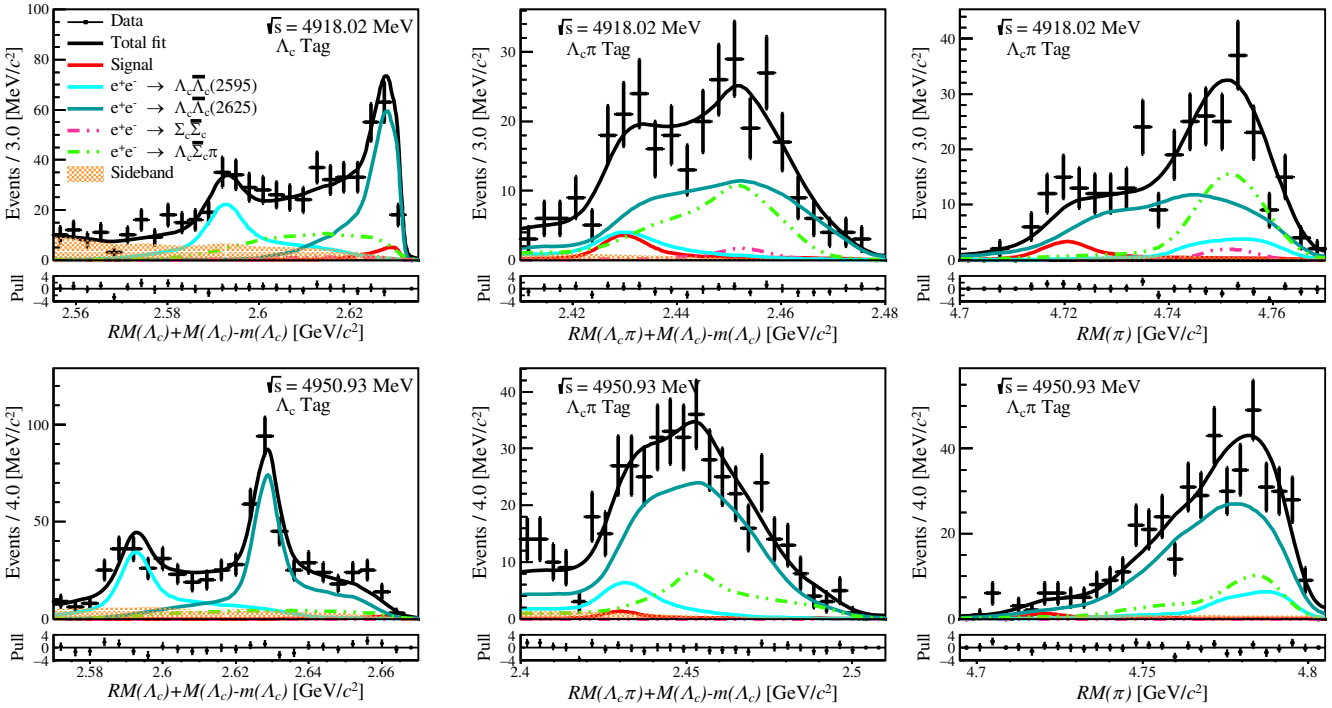


FIG. 2. Simultaneous fit results for H_c with mass of 4720 MeV/c^2 and width of 5 MeV at $\sqrt{s} = 4918.02$ MeV (top) and 4950.93 MeV (bottom). The first column is for the distribution of $RM(\Lambda_c^+) + M(\Lambda_c^+) - m(\Lambda_c^+)$. The second and third columns display the one-dimensional projections of $RM(\Lambda_c^+\pi^\pm) + M(\Lambda_c^+) - m(\Lambda_c^+)$ versus $RM(\pi^\pm)$, respectively. The dots with error bars are data, the black solid curves correspond to the best fit results, the red solid lines show the signal shapes, the cyan solid lines represent the contribution from $e^+e^- \to \Lambda_c\bar{\Lambda}_c(2595)$, the blue solid lines represent the contribution from $e^+e^- \to \Lambda_c\bar{\Lambda}_c(2625)$, the pink dashed lines are the contribution from $e^+e^- \to \Sigma_c\bar{\Sigma}_c$, the green dashed lines are the contribution from $e^+e^- \to \Lambda_c\bar{\Sigma}_c\pi$, the shaded histograms show the Λ_c^+ sideband contributions from each tag's own sideband region.

(b) Contributions from the processes $e^+e^- \to \Sigma_c\bar{\Sigma}_c$, $e^+e^- \to \Lambda_c\bar{\Sigma}_c\pi(\Sigma_c = \Sigma_c^0, \Sigma_c^+,$ and $\Sigma_c^{++})$, $e^+e^- \to \Lambda_c\bar{\Lambda}_c(2595)$, and $e^+e^- \to \Lambda_c\bar{\Lambda}_c(2625)$. These share the same final state $(\pi^+\pi^-\Lambda_c^+\bar{\Lambda}_c^-)$ as the signal process. For $e^+e^- \to \Sigma_c\bar{\Sigma}_c$ and $e^+e^- \to \Lambda_c\bar{\Sigma}_c\pi$, the Born cross sections are unknown and are therefore treated as free parameters in the fit. The Born cross sections for $e^+e^- \to \Lambda_c\bar{\Lambda}_c(2595)$ and $e^+e^- \to \Lambda_c\bar{\Lambda}_c(2625)$ are taken from Ref. [24].

The shapes of background (b) and the signal process are extracted from MC samples. During the simultaneous fitting procedure, the shared parameters are the Born cross sections for the signal and background (b) processes.

The Born cross section for the signal is calculated as follows:

$$\sigma = \frac{N_i^{\rm obs}}{\mathcal{L}_{\rm int} \cdot f_{\rm VP} \cdot f_{\rm ISR} \cdot \mathcal{B} \cdot \epsilon_i}, \quad (1)$$

where $i = 1, 2$ label the "Λ_c Tag" and "$\Lambda_c\pi$ Tag" modes; $N_i^{\rm obs}$ represents the fit yield in each mode and ϵ_i denotes the event selection efficiencies. For all signal MC samples: at $\sqrt{s} = 4918.02$ MeV, ϵ_1 ranges from 17.8% to 18.4% and ϵ_2 ranges from 32.4% to 34.3%; at $\sqrt{s} = 4950.93$ MeV, ϵ_1 ranges from 13.3% to 14.7% and ϵ_2 ranges from 38.0% to 42.1%. $\mathcal{B}$ is the BF of $\Lambda_c^+ \to pK^-\pi^+$, with a value of $(6.28 \pm 0.32)\%$ quoted from the PDG. $\mathcal{L}_{\rm int}$ represents the integrated luminosity. The vacuum polarization factor, $f_{\rm VP}$, is calculated to be 1.056 at the two c.m. energies [25,26]. The ISR correction factor $f_{\rm ISR}$ [27] is obtained using the generator KKMC, yielding values of 1.42 at $\sqrt{s} =$ 4918.02 MeV for all H_c MC samples and 1.55 at $\sqrt{s} = 4950.93$ MeV. The input Born cross sections are assumed to be the same as $e^+e^- \to \Lambda_c\bar{\Lambda}_c$ [28]. For the $e^+e^- \to \Lambda_c\bar{\Lambda}_c^*$ process, the $f_{\rm ISR}$ value is taken from Ref. [24]. Additionally, for the processes $e^+e^- \to \Sigma_c\bar{\Sigma}_c$ and $e^+e^- \to \Lambda_c\bar{\Sigma}_c\pi$ at the two c.m. energies, the $f_{\rm ISR}$ values are 0.90, assuming a flat Born cross section line shape.

The statistical significance of the H_c is estimated by comparing the likelihoods of the fits with and without the inclusion of the signal component. All H_c hypotheses except one have a significance below 3.0σ. For the H_c at a mass of 4720 MeV/c^2 and width of 5 MeV at $\sqrt{s} = 4918.02$ MeV, the significance is 3.0σ. After considering the look elsewhere effect [29] and systematic uncertainty, the significance is less than 2.1σ. The fit results for this H_c are presented in Fig. 2 for both c.m. energies. Additionally, the H_c with mass 4720 MeV/c^2 serves as a representative case in the subsequent discussion on systematic uncertainties. In Sec. V, we determine the upper limits of $\sigma(e^+e^- \to \pi^+H_c^- + \text{c.c.}) \times \mathcal{B}(H_c^- \to \pi^-\Lambda_c^+\bar{\Lambda}_c^-)$ for all H_c hypotheses, taking systematic uncertainties into account.

IV. SYSTEMATIC UNCERTAINTIES

In the cross section measurements, the systematic uncertainties are categorized into multiplicative [(i)–(vi)] and additive terms [(vii)–(ix)], and are assumed to be independent. In Sec. V, we present the upper limit on the signal Born cross section using the Bayesian approach [30]. This method accounts for systematic uncertainties in two stages. Multiplicative systematic uncertainties are incorporated by convolving the likelihood distribution with a Gaussian function. For the additive terms, the largest upper limit of the signal Born cross section from different fit conditions is selected. The summation of the multiplicative terms is shown in Table I. For the additive terms, we describe the methods used to estimate them below.

(1) *Luminosity:* The integrated luminosity for each data sample is measured using Bhabha events, with an uncertainty of 0.7% [7].

(2) *MC statistics:* The systematic uncertainties arising from the finite MC sample sizes are calculated by $\sqrt{(1-\epsilon)/\epsilon}/\sqrt{N}$, where ϵ is the reconstruction efficiency after all the event selection, and N is

TABLE I. The multiplicative systematic uncertainties (in %) for the H_c with a mass of 4720 MeV/c^2 and the widths 5, 10, and 20 MeV at two c.m. energies. The number "$*/*$" refers to the "Λ_c Tag" and the "$\Lambda_c\pi$ Tag," respectively.

c.m. energy (MeV)	4918.02			4950.93		
H_c width (MeV)	5	10	20	5	10	20
Luminosity	0.7					
MC statistics	0.9/0.6			1.0/0.6		
Input BF	5.0					
Tracking and PID	4.3/5.7					
Λ_c^+ vertex fit	2.0					
Mass window of Λ_c^+	2.2	2.1	2.2	1.5	1.5	1.5
Sum for "Λ_c Tag"	7.3	7.3	7.3	7.1	7.1	7.1
Sum for "$\Lambda_c\pi$ Tag"	8.2	8.2	8.2	8.1	8.1	8.1

the number of generated events. At $\sqrt{s} = 4918.02$ MeV, the uncertainties are 0.9% for the "Λ_c Tag" and 0.6% for the "$\Lambda_c\pi$ Tag." At $\sqrt{s} = 4950.93$ MeV, the uncertainties are 1.0% for the "Λ_c Tag" and 0.6% for the "$\Lambda_c\pi$ Tag". These values remain consistent across the H_c widths of 5, 10, and 20 MeV.

(3) *Input BF:* The systematic uncertainty from the BF of $\Lambda_c^+ \to pK^-\pi^+$ is 5.0%.

(4) *Tracking and PID:* The systematic uncertainty due to tracking or PID is assigned as 1.0% for each charged track [31]. They are applied for three tracks in the "Λ_c Tag" ($pK^-\pi^+$) and four tracks in the "$\Lambda_c\pi$ Tag" ($pK^-\pi^+\pi^+$). Therefore, the combined tracking and PID systematic uncertainties for the "Λ_c Tag" and "$\Lambda_c\pi$ Tag" are 4.3% and 5.7%, respectively.

(5) Λ_c^+ *vertex fit:* This systematic uncertainty arises from the difference in the $pK^-\pi^+$ vertex fit efficiencies between the MC simulation and data. Using a control sample of $e^+e^- \to \Lambda_c\bar{\Lambda}_c$, we find a difference of 2.0%, which is taken as the systematic uncertainty.

(6) *Mass window of* Λ_c^+: We use either the direct signal shape or a signal shape convolved with a Gaussian function to fit the data. The proportions of signal events within the Λ_c^+ mass window serve as the resolution for the MC or data, respectively. The difference between these two ratios is regarded as the uncertainty. For $\sqrt{s} = 4918.02$ MeV, the differences for H_c widths of 5, 10, and 20 MeV are 2.2%, 2.1%, and 2.2%, respectively. For $\sqrt{s} = 4950.93$ MeV, the differences are all 1.5%.

(7) *Fit range:* The systematic uncertainty due to the fit range is tested using a Barlow test method [32]. By varying the fit ranges, we find that the change in the signal Born cross section is much less than the statistical uncertainty, so the systematic uncertainties are negligible.

(8) *Signal shape:* The signal MC samples are generated with the Born cross section line shape of $e^+e^- \to \Lambda_c\bar{\Lambda}_c$, as no measurement has been done before. To assess this uncertainty, we vary the line shape to a flat line shape and generate signal MC samples.

(9) *Background:* The two types of background (a) and (b) introduce four sources of systematic uncertainties.

(a) To estimate the uncertainties in the $M(pK^-\pi^+)$ sideband regions from data, we modify these regions to use those derived from the inclusive $e^+e^- \to q\bar{q}$ MC sample.

(b) For the processes $e^+e^- \to \Lambda_c\bar{\Sigma}_c\pi$ and $e^+e^- \to \Sigma_c\bar{\Sigma}_c$, where the cross section line shape is unknown, we assume a flat line shape. To estimate the systematic uncertainty, we alter the line shape from flat to that of $e^+e^- \to \Lambda_c\bar{\Lambda}_c$.

(c) We replace the two original background shapes of $e^+e^- \to \Lambda_c\bar{\Sigma}_c\pi$ and $e^+e^- \to \Sigma_c\bar{\Sigma}_c$ with a single background shape of $e^+e^- \to \Lambda_c\bar{\Sigma}_c\pi$.

(d) For the process $e^+e^- \to \Lambda_c\bar{\Lambda}_c^*$, we use the central Born cross section values from Ref. [24], which has considered the uncertainty in BFs of $\bar{\Lambda}_c^*$. The Born cross sections of this process vary within their error ranges during fitting.

V. RESULT

Due to its low statistical significance, the upper limit on $\sigma(e^+e^- \to \pi^+H_c^- + \text{c.c.}) \times \mathcal{B}(H_c^- \to \pi^-\Lambda_c^+\bar{\Lambda}_c^-)$ is set at a 90% confidence level (CL). To account for systematic uncertainties when determining the upper limit, we define a new likelihood distribution [33] based on the following equation:

$$\tilde{L}(\sigma) = \int L\left(\frac{\epsilon}{\epsilon_0}\sigma\right)\frac{1}{\sqrt{2\pi\sigma_\epsilon^2}}\exp\left[-\frac{(\epsilon-\epsilon_0)^2}{2\sigma_\epsilon^2}\right]d\epsilon, \quad (2)$$

where L is the original likelihood distribution, ϵ_0 represents the nominal selection efficiency, and σ_ϵ denotes the multiplicative systematic uncertainties. Subsequently, the maximum upper limit of the signal Born cross section is

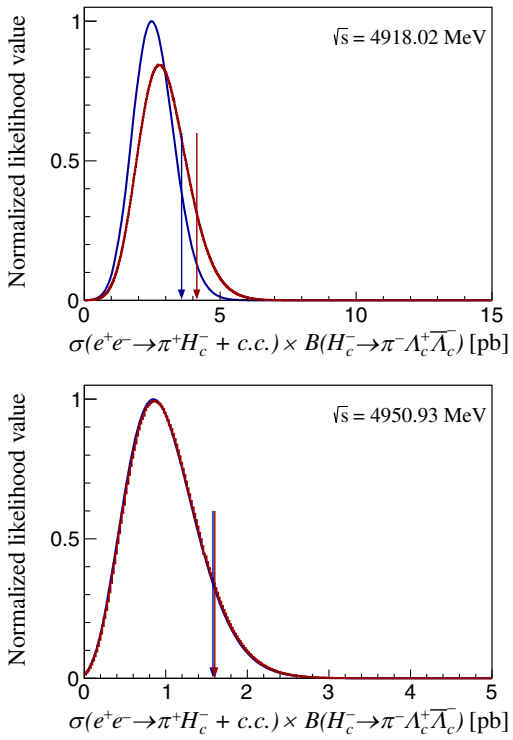


FIG. 3. Distributions of the likelihood versus $\sigma(e^+e^- \to \pi^+H_c^- + \text{c.c.}) \times \mathcal{B}(H_c^- \to \pi^-\Lambda_c^+\bar{\Lambda}_c^-)$ for H_c with mass of 4720 MeV/c^2 and width of 5 MeV at $\sqrt{s} = 4918.02$ MeV (top) and 4950.93 MeV (bottom). The blue and red histograms denote those without and with the incorporation of systematic uncertainties.

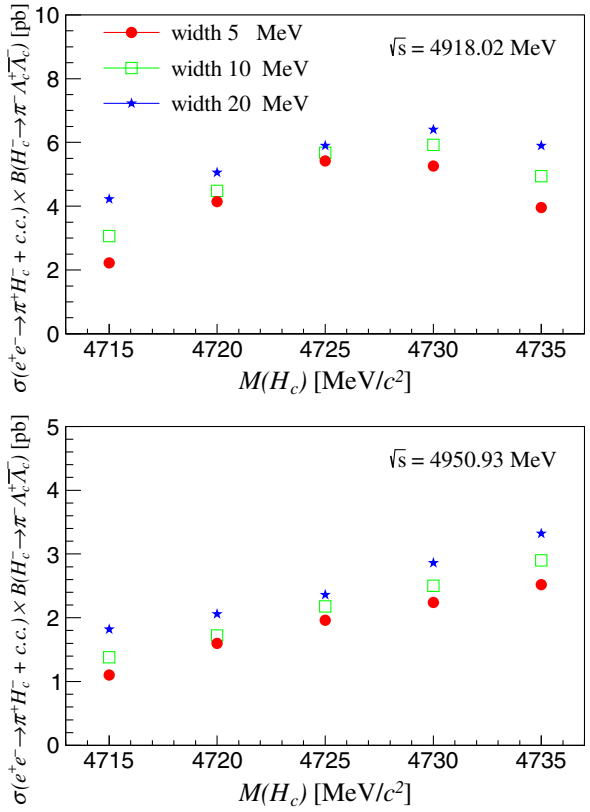


FIG. 4. Upper limits on $\sigma(e^+e^- \to \pi^+ H_c^- + \text{c.c.}) \times \mathcal{B}(H_c^- \to \pi^- \Lambda_c^+ \bar{\Lambda}_c^-)$ at $\sqrt{s} = 4918.02$ MeV (top) and 4950.93 MeV (bottom) for all signal H_c.

determined by taking into account the conditions of various additive systematic terms from different fits. In the simultaneous fit, two likelihoods from the "Λ_c Tag" and "$\Lambda_c\pi$ Tag" are combined multiplicatively to construct the total likelihood. Therefore, the two likelihoods are adjusted using Eq. (2) and then multiplied to derive the total $\tilde{L}$, which is then used to determine the upper limit. As an example, Fig. 3 displays the distributions of the likelihood versus $\sigma(e^+e^- \to \pi^+ H_c^- + \text{c.c.}) \times \mathcal{B}(H_c^- \to \pi^- \Lambda_c^+ \bar{\Lambda}_c^-)$ for the H_c with a mass of 4720 MeV/c^2 and a width of 5 MeV at two c.m. energies. The upper limits on $\sigma(e^+e^- \to \pi^+ H_c^- + \text{c.c.}) \times \mathcal{B}(H_c^- \to \pi^- \Lambda_c^+ \bar{\Lambda}_c^-)$ for all H_c are depicted in Fig. 4, with systematic uncertainties considered.

VI. SUMMARY

In this work, we search for a possible $\Lambda_c\bar{\Sigma}_c$ bound state, denoted H_c, using 208.11 and 160.37 pb^{-1} of e^+e^- annihilation data at $\sqrt{s} = 4918.02$ and 4950.93 MeV, respectively, collected with the BESIII detector. No evidence for this state is observed. We set upper limits on $\sigma(e^+e^- \to \pi^+ H_c^- + c.c) \times \mathcal{B}(H_c^- \to \pi^- \Lambda_c^+ \bar{\Lambda}_c^-)$ at a 90% CL, for the H_c assuming masses of 4715, 4720, 4725, 4730, and 4735 MeV/c^2, and widths of 5, 10, and 20 MeV. The final upper limits, as shown in Fig. 4, range from 1.1 pb to 6.4 pb. This result represents the first search for a $\Lambda_c\bar{\Sigma}_c$ bound state. We note that the background level is high and the data statistics are limited. In the future, the upgraded BEPCII [34] and a next-generation super τ-charm factory [35] could provide more data to identify this signal process.

ACKNOWLEDGMENTS

The BESIII Collaboration thanks the staff of BEPCII [36] and the IHEP computing center for their strong support. This work is supported in part by National Key R&D Program of China under Contracts No. 2023YFA1606000, No. 2023YFA1606704; National Natural Science Foundation of China (NSFC) under Contracts No. 11635010, No. 11935015, No. 11935016, No. 11935018, No. 12025502, No. 12035009, No. 12035013, No. 12061131003, No. 12192260, No. 12192261, No. 12192262, No. 12192263, No. 12192264, No. 12192265, No. 12221005, No. 12225509, No. 12235017, and No. 12361141819; the Chinese Academy of Sciences (CAS) Large-Scale Scientific Facility Program; CAS under Contract No. YSBR-101; 100 Talents Program of CAS; The Institute of Nuclear and Particle Physics (INPAC) and Shanghai Key Laboratory for Particle Physics and Cosmology; ERC under Contract No. 758462; German Research Foundation DFG under Contract No. FOR5327; Istituto Nazionale di Fisica Nucleare, Italy; Knut and Alice Wallenberg Foundation under Contracts No. 2021.0174, No. 2021.0299; Ministry of Development of Turkey under Contract No. DPT2006K-120470; National Research Foundation of Korea under Contract No. NRF-2022R1A2C1092335; National Science and Technology fund of Mongolia; Polish National Science Centre under Contract No. 2024/53/B/ST2/00975; STFC (United Kingdom); Swedish Research Council under Contract No. 2019.04595; U.S. Department of Energy under Contract No. DE-FG02-05ER41374.

DATA AVAILABILITY

The data that support the findings of this article are not publicly available upon publication because it is not technically feasible and/or the cost of preparing, depositing, and hosting the data would be prohibitive within the terms of this research project. The data are available from the authors upon reasonable request.

[1] N. Brambilla, S. Eidelman, C. Hanhart, A. Nefediev, C. P. Shen, C. E. Thomas, A. Vairo, and C. Z. Yuan, Phys. Rep. **873**, 1 (2020).
[2] S. K. Choi *et al.* (BELLE Collaboration), Phys. Rev. Lett. **91**, 262001 (2003).
[3] M. Ablikim *et al.* (BESIII Collaboration), Phys. Rev. Lett. **110**, 252001 (2013).
[4] F. K. Guo, C. Hanhart, U. G. Meißner, Q. Wang, Q. Zhao, and B. S. Zou, Rev. Mod. Phys. **90**, 015004 (2018).
[5] C. F. Qiao, J. Phys. G **35**, 075008 (2008).
[6] X. K. Dong, F. K. Guo, and B. S. Zou, Prog. Phys. **41**, 65 (2021), https://pip.nju.edu.cn/EN/10.13725/j.cnki.pip.2021.02.001.
[7] M. Ablikim *et al.* (BESIII Collaboration), Chin. Phys. C **46**, 113003 (2022).
[8] M. Ablikim *et al.* (BESIII Collaboration), Nucl. Instrum. Methods Phys. Res., Sect. A **614**, 345 (2010).
[9] C. H. Yu *et al.*, in *Proceedings of the 7th International Particle Accelerator Conference* (JACoW Publishing, Geneva, Switzerland, 2016), p. TUYA01.
[10] X. Li *et al.*, Radiat. Detect. Technol. Meth. **1**, 13 (2017).
[11] Y. X. Guo *et al.*, Radiat. Detect. Technol. Meth. **1**, 15 (2017).
[12] P. Cao *et al.*, Nucl. Instrum. Methods Phys. Res., Sect. A **953**, 163053 (2020).
[13] S. Agostinelli *et al.* (GEANT4 Collaboration), Nucl. Instrum. Methods Phys. Res., Sect. A **506**, 250 (2003).
[14] K. X. Huang *et al.*, Nucl. Sci. Tech. **33**, 142 (2022).
[15] S. Jadach, B. F. L. Ward, and Z. Was, Comput. Phys. Commun. **130**, 260 (2000).
[16] D. J. Lange, Nucl. Instrum. Methods Phys. Res., Sect. A **462**, 152 (2001).
[17] R. G. Ping, Chin. Phys. C **32**, 599 (2008).
[18] S. Navas *et al.* (Particle Data Group), Phys. Rev. D **110**, 030001 (2024).
[19] J. C. Chen, G. S. Huang, X. R. Qi, D. H. Zhang, and Y. S. Zhu, Phys. Rev. D **62**, 034003 (2000).
[20] R. L. Yang, R. G. Ping, and H. Chen, Chin. Phys. Lett. **31**, 061301 (2014).
[21] E. Richter-Was, Phys. Lett. B **303**, 163 (1993).
[22] M. Ablikim (BESIII Collaboration), Phys. Rev. Lett. **120**, 029903 (2018).
[23] M. Ablikim *et al.* (BESIII Collaboration), Phys. Rev. Lett. **116**, 052001 (2016).
[24] M. Ablikim *et al.* (BESIII Collaboration), Phys. Rev. D **109**, L071104 (2024).
[25] F. Jegerlehner, Z. Phys. C **32**, 195 (1986).
[26] S. Actis *et al.* (Working Group on Radiative Corrections, Monte Carlo Generators for Low Energies Collaboration), Eur. Phys. J. C **66**, 585 (2010).
[27] S. Jadach, B. F. L. Ward, and Z. Was, Phys. Rev. D **63**, 113009 (2001).
[28] M. Ablikim *et al.* (BESIII Collaboration), Phys. Rev. Lett. **131**, 191901 (2023).
[29] M. Ablikim *et al.* (BESIII Collaboration), Phys. Rev. Lett. **126**, 102001 (2021).
[30] Y. S. Zhu, Chin. Phys. C **32**, 363 (2008).
[31] M. Ablikim *et al.* (BESIII Collaboration), Phys. Rev. Lett. **112**, 251801 (2014).
[32] R. Barlow, arXiv:hep-ex/0207026.
[33] X. X. Liu, X. R. Lü, and Y. S. Zhu, Chin. Phys. C **39**, 103001 (2015).
[34] M. Ablikim *et al.* (BESIII Collaboration), Chin. Phys. C **44**, 040001 (2020).
[35] M. Achasov *et al.*, Front. Phys. **19**, 14701 (2024).
[36] https://cstr.cn/31109.02.BEPC.

M. Ablikim,[1] M. N. Achasov,[4,b] P. Adlarson,[77] X. C. Ai,[82] R. Aliberti,[36] A. Amoroso,[76a,76c] Q. An,[73,59,†] Y. Bai,[58] O. Bakina,[37] Y. Ban,[47,g] H.-R. Bao,[65] V. Batozskaya,[1,45] K. Begzsuren,[33] N. Berger,[36] M. Berlowski,[45] M. Bertani,[29a] D. Bettoni,[30a] F. Bianchi,[76a,76c] E. Bianco,[76a,76c] A. Bortone,[76a,76c] I. Boyko,[37] R. A. Briere,[5] A. Brueggemann,[70] H. Cai,[78] M. H. Cai,[39,j,k] X. Cai,[1,59] A. Calcaterra,[29a] G. F. Cao,[1,65] N. Cao,[1,65] S. A. Cetin,[63a] X. Y. Chai,[47,g] J. F. Chang,[1,59] G. R. Che,[44] Y. Z. Che,[1,59,65] C. H. Chen,[9] Chao Chen,[56] G. Chen,[1] H. S. Chen,[1,65] H. Y. Chen,[21] M. L. Chen,[1,59,65] S. J. Chen,[43] S. L. Chen,[46] S. M. Chen,[62] T. Chen,[1,65] X. R. Chen,[32,65] X. T. Chen,[1,65] X. Y. Chen,[12,f] Y. B. Chen,[1,59] Y. Q. Chen,[35] Y. Q. Chen,[16] Z. Chen,[25] Z. J. Chen,[26,h] Z. K. Chen,[60] J. C. Cheng,[46] S. K. Choi,[10] X. Chu,[12,f] G. Cibinetto,[30a] F. Cossio,[76c] J. Cottee-Meldrum,[64] J. J. Cui,[51] H. L. Dai,[1,59] J. P. Dai,[80] A. Dbeyssi,[19] R. E. de Boer,[3] D. Dedovich,[37] C. Q. Deng,[74] Z. Y. Deng,[1] A. Denig,[36] I. Denysenko,[37] M. Destefanis,[76a,76c] F. De Mori,[76a,76c] B. Ding,[68,1] X. X. Ding,[47,g] Y. Ding,[41] Y. Ding,[35] Y. X. Ding,[31] J. Dong,[1,59] L. Y. Dong,[1,65] M. Y. Dong,[1,59,65] X. Dong,[78] M. C. Du,[1] S. X. Du,[82] S. X. Du,[12,f] Y. Y. Duan,[56] Z. H. Duan,[43] P. Egorov,[37,a] G. F. Fan,[43] J. J. Fan,[20] Y. H. Fan,[46] J. Fang,[1,59] J. Fang,[60] S. S. Fang,[1,65] W. X. Fang,[1] Y. Q. Fang,[1,59] L. Fava,[76b,76c] F. Feldbauer,[3] G. Felici,[29a] C. Q. Feng,[73,59] J. H. Feng,[16] L. Feng,[39,j,k] Q. X. Feng,[39,j,k] Y. T. Feng,[73,59] M. Fritsch,[3] C. D. Fu,[1] J. L. Fu,[65] Y. W. Fu,[1,65] H. Gao,[65] X. B. Gao,[42] Y. Gao,[73,59] Y. N. Gao,[47,g] Y. N. Gao,[20] Y. Y. Gao,[31] S. Garbolino,[76c] I. Garzia,[30a,30b] L. Ge,[58] P. T. Ge,[20] Z. W. Ge,[43] C. Geng,[60] E. M. Gersabeck,[69] A. Gilman,[71] K. Goetzen,[13] J. D. Gong,[35] L. Gong,[41] W. X. Gong,[1,59] W. Gradl,[36] S. Gramigna,[30a,30b] M. Greco,[76a,76c] M. H. Gu,[1,59] Y. T. Gu,[15] C. Y. Guan,[1,65] A. Q. Guo,[32] L. B. Guo,[42] M. J. Guo,[51] R. P. Guo,[50] Y. P. Guo,[12,f] A. Guskov,[37,a] J. Gutierrez,[28] K. L. Han,[65] T. T. Han,[1] F. Hanisch,[3] K. D. Hao,[73,59] X. Q. Hao,[20] F. A. Harris,[67]

K. K. He,[56] K. L. He,[1,65] F. H. Heinsius,[3] C. H. Heinz,[36] Y. K. Heng,[1,59,65] C. Herold,[61] P. C. Hong,[35] G. Y. Hou,[1,65] X. T. Hou,[1,65] Y. R. Hou,[65] Z. L. Hou,[1] H. M. Hu,[1,65] J. F. Hu,[57,i] Q. P. Hu,[73,59] S. L. Hu,[12,f] T. Hu,[1,59,65] Y. Hu,[1] Z. M. Hu,[60] G. S. Huang,[73,59] K. X. Huang,[60] L. Q. Huang,[32,65] P. Huang,[43] X. T. Huang,[51] Y. P. Huang,[1] Y. S. Huang,[60] T. Hussain,[75] N. Hüsken,[36] N. in der Wiesche,[70] J. Jackson,[28] Q. Ji,[1] Q. P. Ji,[20] W. Ji,[1,65] X. B. Ji,[1,65] X. L. Ji,[1,59] Y. Y. Ji,[51] Z. K. Jia,[73,59] D. Jiang,[1,65] H. B. Jiang,[78] P. C. Jiang,[47,g] S. J. Jiang,[9] T. J. Jiang,[17] X. S. Jiang,[1,59,65] Y. Jiang,[65] J. B. Jiao,[51] J. K. Jiao,[35] Z. Jiao,[24] S. Jin,[43] Y. Jin,[68] M. Q. Jing,[1,65] X. M. Jing,[65] T. Johansson,[77] S. Kabana,[34] N. Kalantar-Nayestanaki,[66] X. L. Kang,[9] X. S. Kang,[41] M. Kavatsyuk,[66] B. C. Ke,[82] V. Khachatryan,[28] A. Khoukaz,[70] R. Kiuchi,[1] O. B. Kolcu,[63a] B. Kopf,[3] M. Kuessner,[3] X. Kui,[1,65] N. Kumar,[27] A. Kupsc,[45,77] W. Kühn,[38] Q. Lan,[74] W. N. Lan,[20] T. T. Lei,[73,59] M. Lellmann,[36] T. Lenz,[36] C. Li,[48] C. Li,[44] C. H. Li,[40] C. K. Li,[21] D. M. Li,[82] F. Li,[1,59] G. Li,[1] H. B. Li,[1,65] H. J. Li,[20] H. N. Li,[57,i] Hui Li,[44] J. R. Li,[62] J. S. Li,[60] K. Li,[1] K. L. Li,[20] K. L. Li,[39,j,k] L. J. Li,[1,65] Lei Li,[49] M. H. Li,[44] M. R. Li,[1,65] P. L. Li,[65] P. R. Li,[39,j,k] Q. M. Li,[1,65] Q. X. Li,[51] R. Li,[18,32] S. X. Li,[12] T. Li,[51] T. Y. Li,[44] W. D. Li,[1,65] W. G. Li,[1,†] X. Li,[1,65] X. H. Li,[73,59] X. L. Li,[51] X. Y. Li,[1,8] X. Z. Li,[60] Y. Li,[20] Y. G. Li,[47,g] Y. P. Li,[35] Z. J. Li,[60] Z. Y. Li,[80] C. Liang,[43] H. Liang,[73,59] Y. F. Liang,[55] Y. T. Liang,[32,65] G. R. Liao,[14] L. B. Liao,[60] M. H. Liao,[60] Y. P. Liao,[1,65] J. Libby,[27] A. Limphirat,[61] C. C. Lin,[56] D. X. Lin,[32,65] L. Q. Lin,[40] T. Lin,[1] B. J. Liu,[1] B. X. Liu,[78] C. Liu,[35] C. X. Liu,[1] F. Liu,[1] F. H. Liu,[54] Feng Liu,[6] G. M. Liu,[57,i] H. Liu,[39,j,k] H. B. Liu,[15] H. H. Liu,[1] H. M. Liu,[1,65] Huihui Liu,[22] J. B. Liu,[73,59] J. J. Liu,[21] K. Liu,[39,j,k] K. Liu,[74] K. Y. Liu,[41] Ke Liu,[23] L. C. Liu,[44] Lu Liu,[44] M. H. Liu,[12,f] M. H. Liu,[35] P. L. Liu,[1] Q. Liu,[65] S. B. Liu,[73,59] T. Liu,[12,f] W. K. Liu,[44] W. M. Liu,[73,59] W. T. Liu,[40] X. Liu,[39,j,k] X. Liu,[40] X. K. Liu,[39,j,k] X. L. Liu,[12,f] X. Y. Liu,[78] Y. Liu,[39,j,k] Y. Liu,[82] Yuan Liu,[82] Y. B. Liu,[44] Z. A. Liu,[1,59,65] Z. D. Liu,[9] Z. Q. Liu,[51] X. C. Lou,[1,59,65] F. X. Lu,[60] H. J. Lu,[24] J. G. Lu,[1,59] X. L. Lu,[16] Y. Lu,[7] Y. H. Lu,[1,65] Y. P. Lu,[1,59] Z. H. Lu,[1,65] C. L. Luo,[42] J. R. Luo,[60] J. S. Luo,[1,65] M. X. Luo,[81] T. Luo,[12,f] X. L. Luo,[1,59] Z. Y. Lv,[23] X. R. Lyu,[65,o] Y. F. Lyu,[44] Y. H. Lyu,[82] F. C. Ma,[41] H. L. Ma,[1] Heng Ma,[26,h] J. L. Ma,[1,65] L. L. Ma,[51] L. R. Ma,[68] Q. M. Ma,[1] R. Q. Ma,[1,65] R. Y. Ma,[20] T. Ma,[73,59] X. T. Ma,[1,65] X. Y. Ma,[1,59] Y. M. Ma,[32] F. E. Maas,[19] I. MacKay,[71] M. Maggiora,[76a,76c] S. Malde,[71] Q. A. Malik,[75] H. X. Mao,[39,j,k] Y. J. Mao,[47,g] Z. P. Mao,[1] S. Marcello,[76a,76c] A. Marshall,[64] F. M. Melendi,[30a,30b] Y. H. Meng,[65] Z. X. Meng,[68] G. Mezzadri,[30a] H. Miao,[1,65] T. J. Min,[43] R. E. Mitchell,[28] X. H. Mo,[1,59,65] B. Moses,[28] N. Yu. Muchnoi,[4,b] J. Muskalla,[36] Y. Nefedov,[37] F. Nerling,[19,d] L. S. Nie,[21] I. B. Nikolaev,[4,b] Z. Ning,[1,59] S. Nisar,[11,l] Q. L. Niu,[39,j,k] W. D. Niu,[12,f] C. Normand,[64] S. L. Olsen,[10,65] Q. Ouyang,[1,59,65] S. Pacetti,[29b,29c] X. Pan,[56] Y. Pan,[58] A. Pathak,[10] Y. P. Pei,[73,59] M. Pelizaeus,[3] H. P. Peng,[73,59] X. J. Peng,[39,j,k] Y. Y. Peng,[39,j,k] K. Peters,[13,d] K. Petridis,[64] J. L. Ping,[42] R. G. Ping,[1,65] S. Plura,[36] V. Prasad,[35] F. Z. Qi,[1] H. R. Qi,[62] M. Qi,[43] S. Qian,[1,59] W. B. Qian,[65] C. F. Qiao,[65] J. H. Qiao,[20] J. J. Qin,[74] J. L. Qin,[56] L. Q. Qin,[14] L. Y. Qin,[73,59] P. B. Qin,[74] X. P. Qin,[12,f] X. S. Qin,[51] Z. H. Qin,[1,59] J. F. Qiu,[1] Z. H. Qu,[74] J. Rademacker,[64] C. F. Redmer,[36] A. Rivetti,[76c] M. Rolo,[76c] G. Rong,[1,65] S. S. Rong,[1,65] F. Rosini,[29b,29c] Ch. Rosner,[19] M. Q. Ruan,[1,59] N. Salone,[45,p] A. Sarantsev,[37,c] Y. Schelhaas,[36] K. Schoenning,[77] M. Scodeggio,[30a] K. Y. Shan,[12,f] W. Shan,[25] X. Y. Shan,[73,59] Z. J. Shang,[39,j,k] J. F. Shangguan,[17] L. G. Shao,[1,65] M. Shao,[73,59] C. P. Shen,[12,f] H. F. Shen,[1,8] W. H. Shen,[65] X. Y. Shen,[1,65] B. A. Shi,[65] H. Shi,[73,59] J. L. Shi,[12,f] J. Y. Shi,[1] S. Y. Shi,[74] X. Shi,[1,59] H. L. Song,[73,59] J. J. Song,[20] T. Z. Song,[60] W. M. Song,[35] Y. J. Song,[12,f] Y. X. Song,[47,g,m] Zirong Song,[26,h] S. Sosio,[76a,76c] S. Spataro,[76a,76c] S. Stansilaus,[71] F. Stieler,[36] S. S. Su,[41] Y. J. Su,[65] G. B. Sun,[78] G. X. Sun,[1] H. Sun,[65] H. K. Sun,[1] J. F. Sun,[20] K. Sun,[62] L. Sun,[78] S. S. Sun,[1,65] T. Sun,[52,e] Y. C. Sun,[78] Y. H. Sun,[31] Y. J. Sun,[73,59] Y. Z. Sun,[1] Z. Q. Sun,[1,65] Z. T. Sun,[51] C. J. Tang,[55] G. Y. Tang,[1] J. Tang,[60] J. J. Tang,[73,59] L. F. Tang,[40] Y. A. Tang,[78] L. Y. Tao,[74] M. Tat,[71] J. X. Teng,[73,59] J. Y. Tian,[73,59] W. H. Tian,[60] Y. Tian,[32] Z. F. Tian,[78] I. Uman,[63b] B. Wang,[1] B. Wang,[60] Bo Wang,[73,59] C. Wang,[39,j,k] C. Wang,[20] Cong Wang,[23] D. Y. Wang,[47,g] H. J. Wang,[39,j,k] J. J. Wang,[78] K. Wang,[1,59] L. L. Wang,[1] L. W. Wang,[35] M. Wang,[51] M. Wang,[73,59] N. Y. Wang,[65] S. Wang,[12,f] T. Wang,[12,f] T. J. Wang,[44] W. Wang,[60] Wei Wang,[74] W. P. Wang,[36] X. Wang,[47,g] X. F. Wang,[39,j,k] X. J. Wang,[40] X. L. Wang,[12,f] X. N. Wang,[1,65] Y. Wang,[62] Y. D. Wang,[46] Y. F. Wang,[1,8,65] Y. H. Wang,[39,j,k] Y. J. Wang,[73,59] Y. L. Wang,[20] Y. N. Wang,[78] Y. Q. Wang,[1] Yaqian Wang,[18] Yuan Wang,[18,32] Z. Wang,[1,59] Z. L. Wang,[74] Z. L. Wang,[2] Z. Q. Wang,[12,f] Z. Y. Wang,[1,65] D. H. Wei,[14] H. R. Wei,[44] F. Weidner,[70] S. P. Wen,[1] Y. R. Wen,[40] U. Wiedner,[3] G. Wilkinson,[71] M. Wolke,[77] C. Wu,[40] J. F. Wu,[1,8] L. H. Wu,[1]

L. J. Wu,[1,65] L. J. Wu,[20] Lianjie Wu,[20] S. G. Wu,[1,65] S. M. Wu,[65] X. Wu,[12,f] X. H. Wu,[35] Y. J. Wu,[32] Z. Wu,[1,59] L. Xia,[73,59] X. M. Xian,[40] B. H. Xiang,[1,65] D. Xiao,[39,j,k] G. Y. Xiao,[43] H. Xiao,[74] Y. L. Xiao,[12,f] Z. J. Xiao,[42] C. Xie,[43] K. J. Xie,[1,65] X. H. Xie,[47,g] Y. Xie,[51] Y. G. Xie,[1,59] Y. H. Xie,[6] Z. P. Xie,[73,59] T. Y. Xing,[1,65] C. F. Xu,[1,65] C. J. Xu,[60] G. F. Xu,[1] H. Y. Xu,[68,2] H. Y. Xu,[2] M. Xu,[73,59] Q. J. Xu,[17] Q. N. Xu,[31] T. D. Xu,[74] W. Xu,[1] W. L. Xu,[68] X. P. Xu,[56] Y. Xu,[41] Y. Xu,[12,f] Y. C. Xu,[79] Z. S. Xu,[65] F. Yan,[12,f] H. Y. Yan,[40] L. Yan,[12,f] W. B. Yan,[73,59] W. C. Yan,[82] W. H. Yan,[6] W. P. Yan,[20] X. Q. Yan,[1,65] H. J. Yang,[52,e] H. L. Yang,[35] H. X. Yang,[1] J. H. Yang,[43] R. J. Yang,[20] T. Yang,[1] Y. Yang,[12,f] Y. F. Yang,[44] Y. H. Yang,[43] Y. Q. Yang,[9] Y. X. Yang,[1,65] Y. Z. Yang,[20] M. Ye,[1,59] M. H. Ye,[8,†] Z. J. Ye,[57,i] Junhao Yin,[44] Z. Y. You,[60] B. X. Yu,[1,59,65] C. X. Yu,[44] G. Yu,[13] J. S. Yu,[26,h] L. Q. Yu,[12,f] M. C. Yu,[41] T. Yu,[74] X. D. Yu,[47,g] Y. C. Yu,[82] C. Z. Yuan,[1,65] H. Yuan,[1,65] J. Yuan,[35] J. Yuan,[46] L. Yuan,[2] S. C. Yuan,[1,65] S. H. Yuan,[74] X. Q. Yuan,[1] Y. Yuan,[1,65] Z. Y. Yuan,[60] C. X. Yue,[40] Ying Yue,[20] A. A. Zafar,[75] S. H. Zeng,[64] X. Zeng,[12,f] Y. Zeng,[26,h] Yujie Zeng,[60] Y. J. Zeng,[1,65] X. Y. Zhai,[35] Y. H. Zhan,[60] Shunan Zhang,[71] A. Q. Zhang,[1,65] B. L. Zhang,[1,65] B. X. Zhang,[1] D. H. Zhang,[44] G. Y. Zhang,[20] G. Y. Zhang,[1,65] H. Zhang,[73,59] H. Zhang,[82] H. C. Zhang,[1,59,65] H. H. Zhang,[60] H. Q. Zhang,[1,59,65] H. R. Zhang,[73,59] H. Y. Zhang,[1,59] Jin Zhang,[82] J. Zhang,[60] J. J. Zhang,[53] J. L. Zhang,[21] J. Q. Zhang,[42] J. S. Zhang,[12,f] J. W. Zhang,[1,59,65] J. X. Zhang,[39,j,k] J. Y. Zhang,[1] J. Z. Zhang,[1,65] Jianyu Zhang,[65] L. M. Zhang,[62] Lei Zhang,[43] N. Zhang,[82] P. Zhang,[1,8] Q. Zhang,[20] Q. Y. Zhang,[35] R. Y. Zhang,[39,j,k] S. H. Zhang,[1,65] Shulei Zhang,[26,h] X. M. Zhang,[1] X. Y. Zhang,[41] X. Y. Zhang,[51] Y. Zhang,[1] Y. Zhang,[74] Y. T. Zhang,[82] Y. H. Zhang,[1,59] Y. M. Zhang,[40] Y. P. Zhang,[73,59] Z. D. Zhang,[1] Z. H. Zhang,[1] Z. L. Zhang,[35] Z. L. Zhang,[56] Z. X. Zhang,[20] Z. Y. Zhang,[78] Z. Y. Zhang,[44] Z. Z. Zhang,[46] Zh. Zh. Zhang,[20] G. Zhao,[1] J. Y. Zhao,[1,65] J. Z. Zhao,[1,59] L. Zhao,[1] L. Zhao,[73,59] M. G. Zhao,[44] N. Zhao,[80] R. P. Zhao,[65] S. J. Zhao,[82] Y. B. Zhao,[1,59] Y. L. Zhao,[56] Y. X. Zhao,[32,65] Z. G. Zhao,[73,59] A. Zhemchugov,[37,a] B. Zheng,[74] B. M. Zheng,[35] J. P. Zheng,[1,59] W. J. Zheng,[1,65] X. R. Zheng,[20] Y. H. Zheng,[65,o] B. Zhong,[42] C. Zhong,[20] H. Zhou,[36,51,n] J. Q. Zhou,[35] J. Y. Zhou,[35] S. Zhou,[6] X. Zhou,[78] X. K. Zhou,[6] X. R. Zhou,[73,59] X. Y. Zhou,[40] Y. X. Zhou,[79] Y. Z. Zhou,[12,f] A. N. Zhu,[65] J. Zhu,[44] K. Zhu,[1] K. J. Zhu,[1,59,65] K. S. Zhu,[12,f] L. Zhu,[35] L. X. Zhu,[65] S. H. Zhu,[72] T. J. Zhu,[12,f] W. D. Zhu,[42] W. D. Zhu,[12,f] W. J. Zhu,[1] W. Z. Zhu,[20] Y. C. Zhu,[73,59] Z. A. Zhu,[1,65] X. Y. Zhuang,[44] J. H. Zou,[1] and J. Zu[73,59]

(BESIII Collaboration)

[1]*Institute of High Energy Physics, Beijing 100049, People's Republic of China*
[2]*Beihang University, Beijing 100191, People's Republic of China*
[3]*Bochum Ruhr-University, D-44780 Bochum, Germany*
[4]*Budker Institute of Nuclear Physics SB RAS (BINP), Novosibirsk 630090, Russia*
[5]*Carnegie Mellon University, Pittsburgh, Pennsylvania 15213, USA*
[6]*Central China Normal University, Wuhan 430079, People's Republic of China*
[7]*Central South University, Changsha 410083, People's Republic of China*
[8]*China Center of Advanced Science and Technology, Beijing 100190, People's Republic of China*
[9]*China University of Geosciences, Wuhan 430074, People's Republic of China*
[10]*Chung-Ang University, Seoul, 06974, Republic of Korea*
[11]*COMSATS University Islamabad,*
Lahore Campus, Defence Road, Off Raiwind Road, 54000 Lahore, Pakistan
[12]*Fudan University, Shanghai 200433, People's Republic of China*
[13]*GSI Helmholtzcentre for Heavy Ion Research GmbH, D-64291 Darmstadt, Germany*
[14]*Guangxi Normal University, Guilin 541004, People's Republic of China*
[15]*Guangxi University, Nanning 530004, People's Republic of China*
[16]*Guangxi University of Science and Technology, Liuzhou 545006, People's Republic of China*
[17]*Hangzhou Normal University, Hangzhou 310036, People's Republic of China*
[18]*Hebei University, Baoding 071002, People's Republic of China*
[19]*Helmholtz Institute Mainz, Staudinger Weg 18, D-55099 Mainz, Germany*
[20]*Henan Normal University, Xinxiang 453007, People's Republic of China*
[21]*Henan University, Kaifeng 475004, People's Republic of China*
[22]*Henan University of Science and Technology, Luoyang 471003, People's Republic of China*
[23]*Henan University of Technology, Zhengzhou 450001, People's Republic of China*
[24]*Huangshan College, Huangshan 245000, People's Republic of China*

[25]*Hunan Normal University, Changsha 410081, People's Republic of China*
[26]*Hunan University, Changsha 410082, People's Republic of China*
[27]*Indian Institute of Technology Madras, Chennai 600036, India*
[28]*Indiana University, Bloomington, Indiana 47405, USA*
[29a]*INFN Laboratori Nazionali di Frascati, I-00044, Frascati, Italy*
[29b]*INFN Sezione di Perugia, I-06100, Perugia, Italy*
[29c]*University of Perugia, I-06100, Perugia, Italy*
[30a]*INFN Sezione di Ferrara, I-44122, Ferrara, Italy*
[30b]*University of Ferrara, I-44122, Ferrara, Italy*
[31]*Inner Mongolia University, Hohhot 010021, People's Republic of China*
[32]*Institute of Modern Physics, Lanzhou 730000, People's Republic of China*
[33]*Institute of Physics and Technology, Mongolian Academy of Sciences, Peace Avenue 54B, Ulaanbaatar 13330, Mongolia*
[34]*Instituto de Alta Investigación, Universidad de Tarapacá, Casilla 7D, Arica 1000000, Chile*
[35]*Jilin University, Changchun 130012, People's Republic of China*
[36]*Johannes Gutenberg University of Mainz, Johann-Joachim-Becher-Weg 45, D-55099 Mainz, Germany*
[37]*Joint Institute for Nuclear Research, 141980 Dubna, Moscow region, Russia*
[38]*Justus-Liebig-Universitaet Giessen, II. Physikalisches Institut, Heinrich-Buff-Ring 16, D-35392 Giessen, Germany*
[39]*Lanzhou University, Lanzhou 730000, People's Republic of China*
[40]*Liaoning Normal University, Dalian 116029, People's Republic of China*
[41]*Liaoning University, Shenyang 110036, People's Republic of China*
[42]*Nanjing Normal University, Nanjing 210023, People's Republic of China*
[43]*Nanjing University, Nanjing 210093, People's Republic of China*
[44]*Nankai University, Tianjin 300071, People's Republic of China*
[45]*National Centre for Nuclear Research, Warsaw 02-093, Poland*
[46]*North China Electric Power University, Beijing 102206, People's Republic of China*
[47]*Peking University, Beijing 100871, People's Republic of China*
[48]*Qufu Normal University, Qufu 273165, People's Republic of China*
[49]*Renmin University of China, Beijing 100872, People's Republic of China*
[50]*Shandong Normal University, Jinan 250014, People's Republic of China*
[51]*Shandong University, Jinan 250100, People's Republic of China*
[52]*Shanghai Jiao Tong University, Shanghai 200240, People's Republic of China*
[53]*Shanxi Normal University, Linfen 041004, People's Republic of China*
[54]*Shanxi University, Taiyuan 030006, People's Republic of China*
[55]*Sichuan University, Chengdu 610064, People's Republic of China*
[56]*Soochow University, Suzhou 215006, People's Republic of China*
[57]*South China Normal University, Guangzhou 510006, People's Republic of China*
[58]*Southeast University, Nanjing 211100, People's Republic of China*
[59]*State Key Laboratory of Particle Detection and Electronics, Beijing 100049, Hefei 230026, People's Republic of China*
[60]*Sun Yat-Sen University, Guangzhou 510275, People's Republic of China*
[61]*Suranaree University of Technology, University Avenue 111, Nakhon Ratchasima 30000, Thailand*
[62]*Tsinghua University, Beijing 100084, People's Republic of China*
[63a]*Istinye University, 34010, Istanbul, Turkey*
[63b]*Near East University, Nicosia, North Cyprus, 99138, Mersin 10, Turkey*
[64]*University of Bristol, H H Wills Physics Laboratory, Tyndall Avenue, Bristol BS8 1TL, United Kingdom*
[65]*University of Chinese Academy of Sciences, Beijing 100049, People's Republic of China*
[66]*University of Groningen, NL-9747 AA Groningen, The Netherlands*
[67]*University of Hawaii, Honolulu, Hawaii 96822, USA*
[68]*University of Jinan, Jinan 250022, People's Republic of China*
[69]*University of Manchester, Oxford Road, Manchester M13 9PL, United Kingdom*
[70]*University of Muenster, Wilhelm-Klemm-Strasse 9, 48149 Muenster, Germany*
[71]*University of Oxford, Keble Road, Oxford OX13RH, United Kingdom*
[72]*University of Science and Technology Liaoning, Anshan 114051, People's Republic of China*
[73]*University of Science and Technology of China, Hefei 230026, People's Republic of China*
[74]*University of South China, Hengyang 421001, People's Republic of China*
[75]*University of the Punjab, Lahore-54590, Pakistan*
[76a]*University of Turin, I-10125, Turin, Italy*
[76b]*University of Eastern Piedmont, I-15121, Alessandria, Italy*

[76c]*INFN, I-10125, Turin, Italy*
[77]*Uppsala University, Box 516, SE-75120 Uppsala, Sweden*
[78]*Wuhan University, Wuhan 430072, People's Republic of China*
[79]*Yantai University, Yantai 264005, People's Republic of China*
[80]*Yunnan University, Kunming 650500, People's Republic of China*
[81]*Zhejiang University, Hangzhou 310027, People's Republic of China*
[82]*Zhengzhou University, Zhengzhou 450001, People's Republic of China*

[†]Deceased.
[a]Also at the Moscow Institute of Physics and Technology, Moscow 141700, Russia.
[b]Also at the Novosibirsk State University, Novosibirsk, 630090, Russia.
[c]Also at the NRC "Kurchatov Institute," PNPI, 188300, Gatchina, Russia.
[d]Also at Goethe University Frankfurt, 60323 Frankfurt am Main, Germany.
[e]Also at Key Laboratory for Particle Physics, Astrophysics and Cosmology, Ministry of Education; Shanghai Key Laboratory for Particle Physics and Cosmology; Institute of Nuclear and Particle Physics, Shanghai 200240, People's Republic of China.
[f]Also at Key Laboratory of Nuclear Physics and Ion-beam Application (MOE) and Institute of Modern Physics, Fudan University, Shanghai 200443, People's Republic of China.
[g]Also at State Key Laboratory of Nuclear Physics and Technology, Peking University, Beijing 100871, People's Republic of China.
[h]Also at School of Physics and Electronics, Hunan University, Changsha 410082, China.
[i]Also at Guangdong Provincial Key Laboratory of Nuclear Science, Institute of Quantum Matter, South China Normal University, Guangzhou 510006, China.
[j]Also at MOE Frontiers Science Center for Rare Isotopes, Lanzhou University, Lanzhou 730000, People's Republic of China.
[k]Also at Lanzhou Center for Theoretical Physics, Lanzhou University, Lanzhou 730000, People's Republic of China.
[l]Also at the Department of Mathematical Sciences, IBA, Karachi 75270, Pakistan.
[m]Also at Ecole Polytechnique Federale de Lausanne (EPFL), CH-1015 Lausanne, Switzerland.
[n]Also at Helmholtz Institute Mainz, Staudinger Weg 18, D-55099 Mainz, Germany.
[o]Also at Hangzhou Institute for Advanced Study, University of Chinese Academy of Sciences, Hangzhou 310024, China.
[p]Currently at Silesian University in Katowice, Chorzow, 41-500, Poland.